AIP Applied Physics Letters

Tunable Fano resonance in hybrid graphene-metal gratings

Zhao-xian Chen, Jin-hui Chen, Zi-jian Wu, Wei Hu, Xue-jin Zhang, and Yan-qing Lu

Citation: Applied Physics Letters **104**, 161114 (2014); doi: 10.1063/1.4873541
View online: http://dx.doi.org/10.1063/1.4873541
View Table of Contents: http://scitation.aip.org/content/aip/journal/apl/104/16?ver=pdfcov
Published by the AIP Publishing

Tunable Fano resonance in hybrid graphene-metal gratings

Zhao-xian Chen, Jin-hui Chen, Zi-jian Wu, Wei Hu, Xue-jin Zhang, and Yan-qing Lu[a)]
National Laboratory of Solid State Microstructures and College of Engineering and Applied Sciences, Nanjing University, Nanjing 210093, People's Republic of China

(Received 25 February 2014; accepted 15 April 2014; published online 24 April 2014)

Hybrid graphene-metal gratings with tunable Fano resonance are proposed and theoretically investigated in THz band. The grating contains alternately aligned metal and graphene stripes, which could be viewed as the superposition of two kinds of gratings with the same period. Due to different material properties, the resonance coupling between the metal and graphene parts forms typical Fano-type transmitting spectra. The related physical mechanism is studied by inspecting the induced dipole moment and local surface charge distributions at different wavelengths. Both of the resonance amplitude and frequency of the structure thus are adjustable by tuning graphene's Fermi energy and the grating's geometrical parameters. Furthermore, the Fano-type spectra are also quite sensitive to environmental indices, which supply another kind of tunability. All these features should have promising applications in tunable THz filters, switches, and modulators. © *2014 AIP Publishing LLC*. [http://dx.doi.org/10.1063/1.4873541]

Fano resonance has been a hot topic in plasmonics over recent years for its interesting physics and abundant applications. Fano resonance is named after the Italian physicist Ugo Fano,[1] who gave reasonable explanations to the asymmetric resonance in autoionizing states of atoms. In optics, the first observation of Fano-type lineshape might be Wood's anomalies. Wood's anomalies[2] are not able to be described by Rayleigh's approximation,[3] while they result from the excitation of Sommerfield's type electromagnetic (EM) wave with large tangential momentum on the metallic surface. Fano resonance brings sharp and asymmetric spectrum which arises from the interaction between a discrete narrow state and a wide continuum state.[4] Such resonances are available in various metallic structures and are applicable in switching,[5] slow light,[6] sensing,[7] etc. For example, Fano resonance in asymmetric metamaterials has been applied in ultrasensitive biosensing of monolayers of proteins and their orientations.[7] On the other hand, intentionally tuning the resonance characteristics is also an attractive topic in this field. Heterodimers consisting of mismatched nanoparticles have been demonstrated to enhance the Fano resonance for their ability to tune the dipole and quadruple resonances.[8] Stacking the metamaterial elements vertically is proposed to circumvent the stringent requirements for fabrication and harvest robustness against structure imperfections.[9] Active control of electromagnetically induced transparency in terahertz metamaterials also has been proposed recently by using photoconductive silicon.[10]

Graphene, since its exfoliation from graphite,[11] has become a well-known material with unique optical and electrical properties. As it supports surface plasmons (SPs) with both high confinement and relatively low loss,[12] graphene shows some advantages over metals for plasmonics devices,[13] especially in infrared and terahertz spectral range. What's more, with electrical gating and doping, graphene further shows interesting tunability which provides an effective way to manipulate the interaction between photons and graphene. So far, graphene has been extensively studied for applications in Terahertz laser,[14] plasmonic waveguide,[15] absorber,[16] and plasmonic metamaterials.[17,18] It would be interesting to adopt graphene in these tunable plasmonic and photonic systems including Fano resonance.[18]

In this Letter, we come up with a controllable structure for Fano resonance. It consists of hybrid graphene-metal (G/M) gratings on a dielectric substrate. Metal grating with high ohmic loss provides a broad spectrum, while graphene grating with low loss offers a narrow discrete resonance. Interactions between them result in Fano resonance and generate transmitting spectra with sharp and asymmetric spectral line profiles. Resonance transition between heterogeneous gratings is studied to reveal the physical mechanism behind the Fano resonance which is controllable by adjusting the geometry parameters and graphene's electric responses. The structure has quite high tolerance in dimensions to withstand the fabrication flaws, but it is quite sensitive to the environmental index which provides an effective way for spectrum control. Electro-optical polymer or liquid crystal thus could be used to further tune the resonance wavelengths.[19] Other interesting phenomena, such as Wood's anomalies of the corresponding structure also have been studied. We believe the Fano resonance in the G/M gratings will trigger various interesting applications in THz communication and biosensor.

Figure 1 shows the proposed structure with evident Fano resonance, which consists of a hybrid G/M grating. Widths of the graphene and metal stripes are W_{GR} and W_{ME}, respectively. The grating period is W and widths of the two gaps between adjacent stripes are W_1 and W_2, respectively. Refractive indices of the substrate and cladding are n_2 and n_1, respectively. Gratings are along the y-direction and are shined with a plane wave. Wave number k is against z-direction and the electric field is polarized along x-direction.

We use the well-known Kubo formula to derive the surface conductivity of the graphene sheet and the formula is[20]

[a)]Electronic mail: yqlu@nju.edu.cn.

$$\sigma_{GR} = \frac{ie^2}{4\pi\hbar} In\left[\frac{2|Ef| - (\omega + i2\Gamma)\hbar}{2|Ef| + (\omega + i2\Gamma)\hbar}\right] + \frac{ie^2 k_B T}{\pi\hbar^2(\omega + i2\Gamma)} \times \left[\frac{Ef}{k_B T} + 2In(e^{-Ef/k_B T} + 1)\right]. \quad (1)$$

In this formula, e, ħ, and k_B are universal constants; ω is the angular frequency of the electromagnetic field. Ef is the Fermi energy and Γ is the intrinsic losses relating to the electro-phonon relaxation time τ ($2\Gamma = \hbar/\tau$). We set the temperature T at 300 K. For highly doped graphene at THz range, only intraband electron transition, i.e., the second term in Eq. (1), has the major contribution, then the surface conductivity could be simplified as[21]

$$\sigma_{GR} = \frac{ie^2 Ef}{\pi\hbar(\hbar\omega + i2\Gamma)}. \quad (2)$$

We also assume the graphene sheet has the thickness of $\Delta = 1$ nm, and the permittivity can be derived from $\varepsilon_{GR} = \varepsilon_0 + i\sigma_{GR}/(\omega\Delta)$.

To begin with, we study the transmittance of a pure metal grating with $W = 15\,\mu m$, $W_{ME} = 8\,\mu m$, and $n_1 = n_2 = 3.5$. Its transmitting spectrum is plotted in Fig. 1(b). The spectrum (red dashed curve) is quite broad and the grating is almost transparent at low frequency range. For frequency around 5.7 THz, there is a dip in the spectrum, which just shows a typical Wood's anomalies.[2] The anomaly results from the excitation of surface wave with momentum on the metal surface. Such surface wave is a kind of plasmon resonance and damps strongly in the transversal direction.[1] For a pure graphene grating with the same period, the other parameters are $W_{GR} = 3\,\mu m$, $Ef = 1.2$ eV, and $\Gamma = 0.1$ meV, respectively. As the green dashed curve shows, there are several dips in graphene grating transmitting spectrum which are caused by the exciting of SPs resonance in graphene stripes. The dip at 3.45 THz is caused by the fundamental mode, and in this case the graphene stripes possess dipole-like charge distributions. For frequency larger than 6 THz, graphene stripes support higher order modes but the resonances are weak. As a result, these dips are much shallower. For a hybrid G/M grating which is the combination of the graphene and metal gratings, asymmetric Fano-type spectrum emerges as shown with the blue solid curve in Fig. 1(b) as well. We set $W_1 = W_2$, and comparison between these three spectra tells the mechanism behind the Fano resonance. The metal grating provides a broad spectrum and the graphene grating provides narrow spectra at resonance frequencies. As a result, SPs in low-loss graphene part couple with those in high-loss metal part which leads to a Fano-type spectral profile.

In order to understand the mechanism behind the Fano-type resonance of hybrid gratings, dipole moments (DMs) of the graphene and metal stripes are calculated and shown in Fig. 2(a). Parameters are the same as the case in Fig. 1(b) and the incident wave intensity keeps constant to normalize the DMs. Charges are generated on the G/M stripes and originated from the difference between electric displacement vectors on a stripe's two sides. Absolute value of the graphene stripes' DMs (green curve) increases greatly around the resonance frequency but with opposite signs. On the contrary, absolute values of metal part's DMs decrease drastically which is caused by the excitation of some electric multipoles. Away from the resonance frequency, DMs of graphene grating are much smaller than those of metal grating because SPs are not efficiently excited in graphene grating. All these phenomena result from the different EM responses and interactions of SPs in metal and graphene stripes.

The transmission phase reflects the abrupt phase change due to the surface grating structure, which is shown in Fig. 2(b). It exhibits a typical resonance spectral line-shape as well. If the grating period is much smaller than the incident wavelength, charges in the stripes instantaneously follow the electric field. The phase change is π as predicted in the figure. To further reveal the origin of the induced dipole nature on the grating, Fig. 2(c) shows the normalized surface charge distributions in the stripes' cross section at certain frequencies. The corresponding wavelengths are also marked in Figs. 2(a) and 2(b). These obtained charge distributions coincides with the spectral trend of the overall dipoles we just discussed. If the frequency is much smaller than the resonance frequency of graphene grating, DM of graphene part is much weaker than its metal counterpart representing by point A. Comparing the surface charge distributions at points B, C, and D clearly shows the destructive interaction between SPs in the gratings. DM of the metal part is much stronger than that of the graphene one at point E which is again far away from the resonance frequency.

We then study the tunability of the Fano resonance in this hybrid G/M grating. To study the influence of graphene stripes' parameters, W_{GR} is varied from $1\,\mu m$ to $4\,\mu m$ and other parameters are set at $W = 15\,\mu m$, $W_{ME} = 8\,\mu m$, $W_1 = W_2$, $Ef = 1.4$ eV, and $\Gamma = 0.1$ meV. As shown in Fig. 3(a), Fano resonance frequency roughly matches the graphene grating's resonance frequency and decreases together with W_{GR}. This tendency can be explained from the condition to excite graphene SPs. Resonating SPs in graphene part demands $W_{GR} \sim n \times \lambda_{GSP}/2$,[22] where n is an integer and λ_{GSP} is the SPs wavelength. Considering the

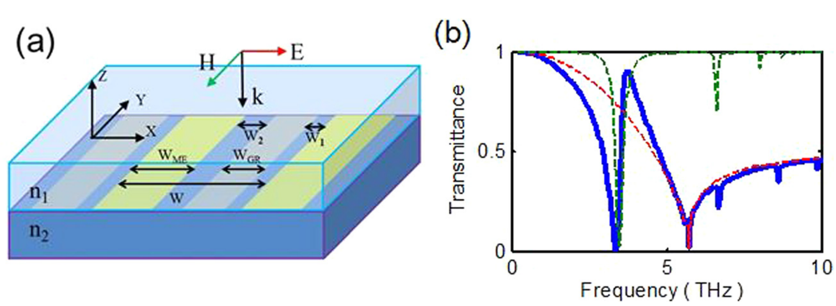

FIG. 1. (a) Scheme of a hybrid G/M grating. Geometry parameters are denoted above and the plane wave is incident against z-direction with its electric field polarized along the x-direction. (b) Transmittance of a hybrid G/M grating (blue), graphene grating (green), and a metal grating (red). Parameters are $W = 15\,\mu m$, $W_{ME} = 8\,\mu m$, $W_{GR} = 3\,\mu m$, $W_1 = W_2 = 3\,\mu m$, $n_1 = n_2 = 3.5$, $Ef = 1.2$ eV, and $\Gamma = 0.1$ meV.

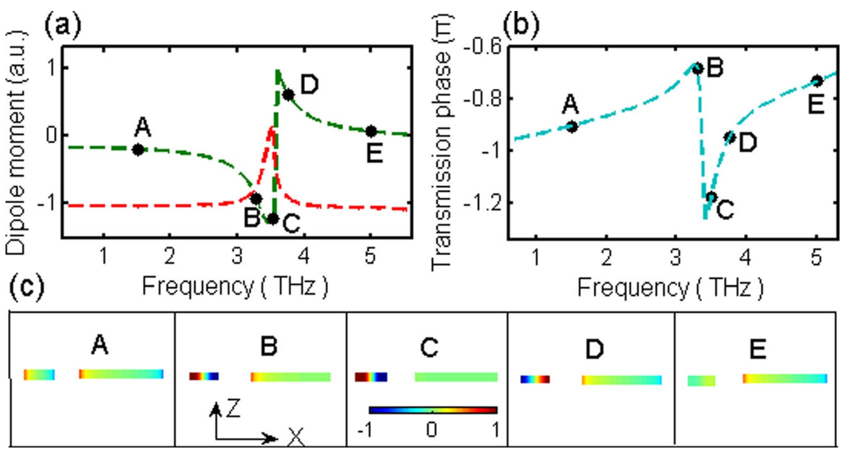

FIG. 2. (a) DMs of graphene stripes (green) and metal stripes (red), respectively. (b) Transmission phase of hybrid gratings. (c) Surface charge distributions inside a unit cell at frequencies: 1.5, 3.3, 3.5, 3.75, and 5 THz shown in (a). Parameters are $W = 15\,\mu m$, $W_{ME} = 8\,\mu m$, $W_{GR} = 3\,\mu m$, $W_1 = W_2$, $Ef = 1.2\,eV$, and $\Gamma = 0.1\,meV$.

property of SPs on graphene,[15] the resonance frequency is obtained as $f_{RES} \propto \sqrt{Ef/W_{GR}}$. For $W_{GR} = 1\,\mu m$, the Fano resonance frequency is even higher than the Wood's anomaly point. Larger W_{GR} would shift the Fano resonance to lower frequencies where graphene is more absorptive. As a result, the Fano-type resonant spectrum becomes broader.

Figure 3(b) shows the response of the Fano resonance to graphene's Fermi energy Ef. In this simulation, Ef varies from 0.4 eV to 1.6 eV with other parameters set as $W = 15\,\mu m$, $W_{ME} = 8\,\mu m$, $W_{GR} = 1\,\mu m$, $W_1 = W_2$, and $\Gamma = 0.1\,meV$. Fano resonance frequency thus is tunable within a large range and increases with Ef, agreeing with the estimated f_{RES} introduced above. Interestingly, no obvious Fano resonance occurs if the resonance frequency of graphene's SPs matches Wood's anomaly point. This is because the line shape of the Wood's anomaly is too narrow thus the coupling between these two kinds of SPs deteriorates.

The performance tolerance of our structure is also a valuable feature in practical applications, which has been studied with the results shown in Figs. 3(c) and 3(d). To investigate the impact of graphene's intrinsic loss, we set $W = 15\,\mu m$, $W_{ME} = 8\,\mu m$, $W_{GR} = 1\,\mu m$, $W_1 = W_2$, and $Ef = 0.8\,eV$. Reducing Γ extends electro-phonon relaxation time τ and enlarges graphene's conductivity. Consequently, interaction between SPs in the gratings is strengthened and the Fano resonance line shape becomes sharper. As far as fabrication is concerned, widths of gaps between graphene and metal gratings are not easy to control. To represent the influence of fabrication flaws, parameters are set at $W = 15\,\mu m$, $W_{ME} = 8\,\mu m$, $W_{GR} = 2\,\mu m$, $Ef = 1.2\,eV$, and $\Gamma = 0.1\,meV$. Now, the sum of the two gaps is $W_1 + W_2 = 5\,\mu m$ and the transmittance spectrum almost remains unchanged when W_1 varies from $0.5\,\mu m$ to $2.5\,\mu m$. As the SPs resonance of the metal grating and graphene grating are all collective response to the applied electric field, they always may interact with each other well no matter how these two sets of gratings locate.

At last, we would study the influence of the environmental conditions. Normally, the grating could be exposed in air or immersed in any liquid. It also could be covered with another "solid" dielectric layer. We assume the refractive index of the cladding changes from 1 to 2, which covers the achievable tuning ranges of liquid crystals and electro-optic polymers. Other parameters are $n_2 = 3.5$, $W = 15\,\mu m$, $W_{ME} = 8\,\mu m$, $W_{GR} = 1\,\mu m$, $W_1 = W_2$, $Ef = 1.2\,eV$, and $\Gamma = 0.1\,meV$. As shown in Fig. 4(a), larger difference between n_1 and n_2 results in stronger reflection and smaller n_1 leads to smaller transmittance. As n_1 does not affect the transmitting refraction, there is always a Wood's anomaly point near 5.7 THz. For $n_1 = 2$, another Wood's anomaly point emerges at 10 THz as reflective diffraction occurs. Response of Fano resonance with n_1 is shown in Fig. 4(b). Dip position of the first order Fano resonance varies linearly with n_1 and ranges between 4.1 and 4.5 THz. Meanwhile,

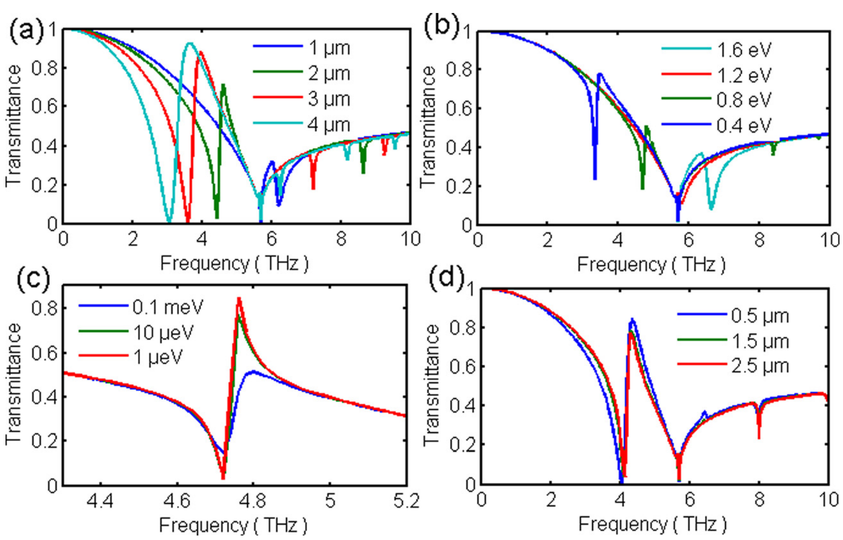

FIG. 3. (a) Transmittance of the hybrid gratings for different W_{GR} with $W = 15\,\mu m$, $W_{ME} = 8\,\mu m$, $W_1 = W_2$, $Ef = 1.4\,eV$, and $\Gamma = 0.1\,meV$. (b) Transmittance of the hybrid gratings for different Ef with $W = 15\,\mu m$, $W_{ME} = 8\,\mu m$, $W_{GR} = 1\,\mu m$, $W_1 = W_2$, and $\Gamma = 0.1\,meV$. (c) Transmittance of the hybrid gratings for different Γ with $W = 15\,\mu m$, $W_{ME} = 8\,\mu m$, $W_{GR} = 1\,\mu m$, $W_1 = W_2$, and $Ef = 0.8\,eV$. (d) Transmittance of the hybrid gratings for different W_1 ($W_1 + W_2 = 5\,\mu m$) with $W = 15\,\mu m$, $W_{ME} = 8\,\mu m$, $W_{GR} = 2\,\mu m$, $Ef = 1.2\,eV$, and $\Gamma = 0.1\,meV$.

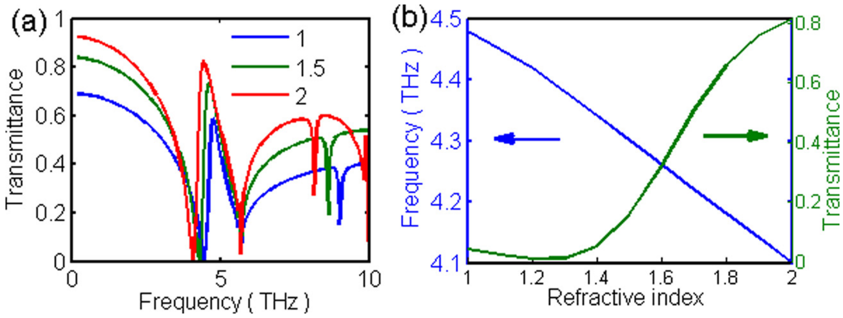

FIG. 4. (a) Transmittance of the hybrid gratings for different n_1 with $W = 15\,\mu m$, $W_{ME} = 8\,\mu m$, $W_{GR} = 1\,\mu m$, $W_1 = W_2$, $Ef = 1.2\,eV$, and $\Gamma = 0.1\,meV$. (b) Blue curve is the position of the Fano dip for different n_1 and dark green curve is transmittance at 4.4 THz. Other parameters are the same as (a).

transmittance at 4.4 THz varies from 0 to 0.8. We further evaluate our system with the "figure of merit" (FOM) introduced by Sherry *et al*. to qualify the sensitivity to environment.[23] The FOM is defined as the shift of the resonance per refractive index unit divided by the resonance width. According to Fig. 4, FOM of the first Fano resonance is smaller than 1, but FOM of the second one is about 7. As Fano resonance width decreases with graphene stripes' width and Fermi level according to Fig. 3, it is possible to get a FOM larger than 10 which shows great advantages over other Fano resonance systems such as nanoparticle resonance.[23,24] This sensitivity supplies an effective approach to further tune the Fano resonance. Interesting applications would be expected in THz sensing and communications.

In summary, we proposed and investigated hybrid graphene-metal gratings with tunable Fano resonance. The resonance results from the interaction between different SPs in graphene and metal gratings. Graphene used here provides great tunability for the Fano resonance frequency and amplitude. The structure is quite robust to withstand the mechanical mismatches between two gratings but it is quite sensitive to the environment refractive index. The related applications of this hybrid grating are also addressed.

This work was sponsored by 973 programs (Nos. 2011CBA00205 and 2012CB921803), the National Science Fund for Distinguished Young Scholars with Contract No. 61225026 and the Program for Changjiang Scholars and Innovative Research Team in University with Contact No. IRT13021.

[1]U. Fano, J. Opt. Soc. Am. **31**(3), 213 (1941).
[2]R. W. Wood, Philos. Mag. Ser. 6 **4**(21), 396 (1902).
[3]Lord Rayleigh, Philos. Mag. Ser. 6 **14**(79), 60 (1907).
[4]B. Luk'yanchuk, N. I. Zheludev, S. A. Maier, N. J. Halas, P. Nordlander, H. Giessen, and C. T. Chong, Nature Mater. **9**(9), 707 (2010).
[5]Z. L. Sámson, K. F. MacDonald, F. De Angelis, B. Gholipour, K. Knight, C. C. Huang, E. Di Fabrizio, D. W. Hewak, and N. I. Zheludev, Appl. Phys. Lett. **96**(14), 143105 (2010).
[6]N. Papasimakis and N. I. Zheludev, Opt. Photonics News **20**(10), 22 (2009).
[7]C. Wu, A. B. Khanikaev, R. Adato, N. Arju, A. A. Yanik, H. Altug, and G. Shvets, Nature Mater. **11**(1), 69 (2012).
[8]L. V. Brown, H. Sobhani, J. B. Lassiter, P. Nordlander, and N. J. Halas, ACS Nano **4**(2), 819 (2010).
[9]N. Liu, L. Langguth, T. Weiss, J. Kastel, M. Fleischhauer, T. Pfau, and H. Giessen, Nature Mater. **8**(9), 758 (2009).
[10]J. Q. Gu, R. J. Singh, X. J. Liu, X. Q. Zhang, Y. F. Ma, S. Zhang, S. A. Maier, Z. Tian, A. K. Azad, H. T. Chen, A. J. Taylor, J. G. Han, and W. L. Zhang, Nat. Commun. **3**, 1151 (2012).
[11]K. S. Novoselov, A. K. Geim, S. V. Morozov, D. Jiang, Y. Zhang, S. V. Dubonos, I. V. Grigorieva, and A. A. Firsov, Science **306**(5696), 666 (2004).
[12]W. B. Lu, W. Zhu, H. J. Xu, Z. H. Ni, Z. G. Dong, and T. J. Cui, Opt. Express **21**(9), 10475 (2013).
[13]X. G. Luo, T. Qiu, W. B. Lu, and Z. H. Ni, e-print arXiv:1309.3654v2 (2013).
[14]V. V. Popov, O. V. Polischuk, A. R. Davoyan, V. Ryzhii, T. Otsuji, and M. S. Shur, Phys. Rev. B **86**(19), 195437 (2012).
[15]A. Vakil and N. Engheta, Science **332**(6035), 1291 (2011).
[16]S. Thongrattanasiri, F. H. L. Koppens, and F. J. G. de Abajo, Phys. Rev. Lett. **108**(4), 047401 (2012).
[17]Z. Y. Fang, Z. Liu, Y. M. Wang, P. M. Ajayan, P. Nordlander, and N. J. Halas, Nano Lett. **12**(7), 3808 (2012); S. H. Lee, M. Choi, T. T. Kim, S. Lee, M. Liu, X. B. Yin, H. K. Choi, S. S. Lee, C. G. Choi, S. Y. Choi, X. Zhang, and B. Min, Nature Mater. **11**(11), 936 (2012).
[18]N. K. Emani, T. F. Chung, A. V. Kildishev, V. M. Shalaev, Y. P. Chen, and A. Boltasseva, Nano Lett. **14**(1), 78 (2014); N. Papasimakis, Z. Q. Luo, Z. X. Shen, F. D. Angelis, E. D. Fabrizio, A. E. Nikolaenko, and N. I. Zheludev, Opt. Express **18**(8), 8353 (2010).
[19]X. W. Lin, J. B. Wu, W. Hu, Z. G. Zheng, Z. J. Wu, G. Zhu, F. Xu, B. B. Jin, and Y. Q. Lu, AIP Adv. **1**(3), 032133 (2011).
[20]V. P. Gusynin, S. G. Sharapov, and J. P. Carbotte, J. Phys.: Condens. Matter **19**(2), 026222 (2007).
[21]G. W. Hanson, J. Appl. Phys. **104**(8), 084314 (2008).
[22]A. Y. Nikitin, F. Guinea, F. J. García-Vidal, and L. M. Moreno, Phys. Rev. B **84**(16), 161407 (2011).
[23]L. J. Sherry, S.-H. Chang, G. C. Schatz, and R. P. Van Duyne, Nano Lett. **5**(10), 2034–2038 (2005).
[24]N. A. Mirin, K. Bao, and P. Nordlander, J. Phys. Chem. A **113**, 4028 (2009).